ADDIS ABABA LIGHT RAIL TRANSIT SYSTEM ENERGY FLOW ANALYSIS

Asegid Belay [1] and Getachew Biru [2]

[1] African Railway Center of Excellence, Addis Ababa Institute of Technology, AAU

[2] School of Electrical & Computer Engineering, Addis Ababa Institute of Technology, AAU
Corresponding Author's Email: Assegidjesus@gmail.com

ABSTRACT

With the continued focus on growing energy prices and environmental concerns, lowering energy consumption and maintaining the environmental sustainability of railway systems is becoming a crucial problem to which greater attention is being paid. In recent years, urban rail systems have grown in popularity as a method for reducing traffic congestion and pollution in metropolitan areas. Despite the fact that the railway system is likely the most energy-efficient mode of land-based transportation, there is still potential for improvement. In this regard, significant amounts of energy can be saved by installing energy storage on an electrified transit system allowing energy from braking to be captured. However, the amount of energy saved is dependent on the amount of energy transferred during braking, which relies on the drive cycle and the vehicle parameters. The overall benefit can be determined by analyzing the energy flow through components in an electrified transit system. In this paper, electrified transit system energy flows are analyzed for Addis Ababa light rail transit system. The methodology used assesses energy flows in the traction system, establishing where energy is dissipated. The analysis is performed for a specified drive cycle. Finally, the analysis showed that 37.9 % of the total energy loss over a drive cycle could be saved in Addis Ababa light rail transit system.

Keywords: braking energy, energy flow, energy efficiency, environmental sustainability, light rail transit,

INTRODUCTION

Today, there is a growing emphasis on the environmental consequences of all government initiatives and policies. Sustainability is becoming increasingly important as people have a better understanding of the reactive changes and deterioration of planet Earth that we are experiencing on daily basis. As Rohit Sharma and Peter Newman sustainability is defined as "development that fulfills current demands without jeopardizing future generations' ability to meet their own needs." Ultimately, the sustainable development method is the only way that humanity can pursue for future generations. Without it, the earth's natural resources will be gone, leaving only synthetic materials. These options involve a system of boundaries in time (25–50 years), space (micro and macro-levels), and domain (social, economic, and environment) [2].

Sustainability is also an important factor in the construction of rail transportation. As governments look to the future for sustainable transportation, electrified rail networks have given and will continue to provide a mode that uses renewable energy. According to studies, rail is naturally more efficient than road transport, and when combined with renewable energy, it may provide a long-term source of mobility for future generations while reducing emissions [3]. Today, it is apparent that urban rail systems play an important role in the sustainable development of metropolitan cities like Addis Ababa for a variety of reasons, the most important of which is their relatively low energy consumption to transit capacity ratio. Nonetheless, major improvements in energy efficiency are required to maintain their environmental benefits over other modes of transportation in a context defined by increasing capacity demands and energy prices. There is widespread consensus that railways have significant energy savings potential, both short and long terms. Whereas technology advancements in rail cars will be gradual and take time to diffuse, there are

numerous viable short and medium-term saving techniques targeted at optimal control and the utilization of current technologies or operational enhancements. Consequently, energy efficiency has emerged as a prominent subject within railway industry. For example, 28 European railway Operators have committed to reduce CO_2 emissions per passenger kilometer and per ton kilometer by 50% by 2030 [4].

In addition to improvements in vehicle technology, infrastructure and building design, and loading of freight trains, the European union commissioned study [5] identifies several potential areas, which can achieve efficiency improvements in railway systems such as weight reduction, reduction of air resistance, optimization of space utilization, improvements in electric traction components, efficiency gains in diesel traction technology, recovery of braking energy, reduction in energy consumption of comfort functions, energy efficient driving, traffic flow management, improvement of occupancy rates, energy meters and management and organization.

All these areas can be investigated to achieve energy efficiency improvements. It is also essential to consider the interactions between the different areas, particularly when efficiency gains are achieved by installing components, which increase the weight of electric vehicles and affect space utilization. On the other hand, recently energy flow assessment has gained huge momentum in railway system. Research undertaken in [6] performed a comprehensive analysis to determine where energy is dissipated in traction system.

The result consists of an analysis of energy movements into and out of trains as shown in Fig.1, taking into account losses. This research paper developed methods used to analyses energy flows in Addis Ababa light rail electrified transit system. The analysis is used to assess the energy dissipated through braking, hence establishing the amount of energy that could be potentially saved.

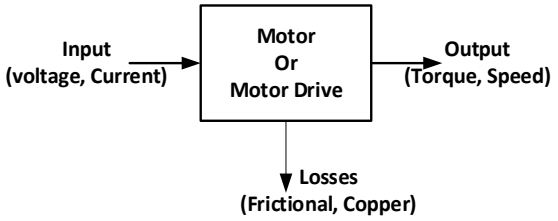

Fig.1 Energy flow block diagram

Energy flow in light rail transit

An electric transit vehicle converts electrical energy into kinetic and potential energy. Energy is dissipated overcoming frictional forces and in braking. Energy is also dissipated through other mechanisms, including driveline losses and to power auxiliary loads. The electrical energy is transmitted from a local distribution network, through a traction substation, and the traction supply system. These stages also have energy losses. Fig.2 shows a more comprehensive representation of energy flows in an electrified transit system, including loss mechanisms. This paper considers the energy flow through each sub system identified in Fig.2 determine the overall energy dissipation.

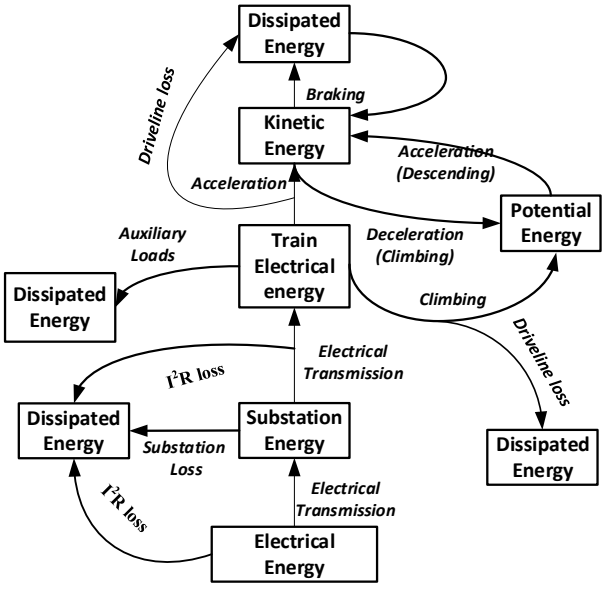

Fig.2 Energy flow in railway system

Tractive resistance

In all traction applications, energy is consumed overcoming frictional forces. Davis [7] describes tractive resistance, F_R as a quadratic function of the speed of a vehicle.

$$F_R = a + b\left(\frac{ds}{dt}\right) + c\left(\frac{ds}{dt}\right)^2 \quad (1)$$

The first term a, is a constant with respect to speed (except at zero speed) but varies with the mass of the vehicle. The constant term is made up of two components, journal resistance and the static component of rolling resistance. The second term, ds/dt includes resistive forces which are proportional to speed, including the dynamic component of rolling resistance. The third term $(ds/dt)^2$ represents aerodynamic drag forces. Curvature resistance adds another element to tractive resistance, however this can be considered negligible. The coefficients of the Davis equation can be calculated by considering the laws of physics, taking into account aerodynamic drag, rolling resistance and static friction. The parameters are often determined experimentally [8], fitting the coefficients to curves obtained through run-down tests. If the velocity of a vehicle is considered as a function of time, $ds(t)/dt$, the resistive force can be described as a function of time $F_R(t)$,

$$F_R(t) = a + b\left(\frac{ds(t)}{dt}\right) + c\left(\frac{ds(t)}{dt}\right)^2 \quad (2)$$

The Power, $P_R(t)$ dissipated by the train to overcome a frictional force is the product of force and speed,

$$P_R(t) = F_R(t).\frac{ds(t)}{dt} \quad (3)$$

Then using (2) and (3)

$$P_R(t) = a\frac{ds(t)}{dt} + b\left(\frac{ds(t)}{dt}\right)^2 + c\left(\frac{ds(t)}{dt}\right)^3 \quad (4)$$

This can be integrated with respect to time to determine the energy losses caused by frictional forces.

$$E_R(t) = \int_{to}^{t} a\frac{ds(t)}{dt} + b\left(\frac{ds(t)}{dt}\right)^2 + c\left(\frac{ds(t)}{dt}\right)^3 \quad (5)$$

The driveline

The typical energy flow diagram via the DC-fed railway is illustrated in Fig. 2 to evaluate the overall energy efficiency of the system from the substation to the train. In terms of levels, there are three layers: substation level, catenary system level, and train level. The substations take electricity from the national power grid to power the whole railway system. After losses from substations, the remaining substation energy can be transmitted to the catenary. Some energy is wasted as heat when the current passes through the resistive catenary wire. The resistance of the transmission conductor is a time-varying parameter determined by the position of the trains and the network. The train receives energy through its pantograph. Finally, energy reaches to the traction motors through mechanical transmission system and power electronics converter as shown in Fig.3.

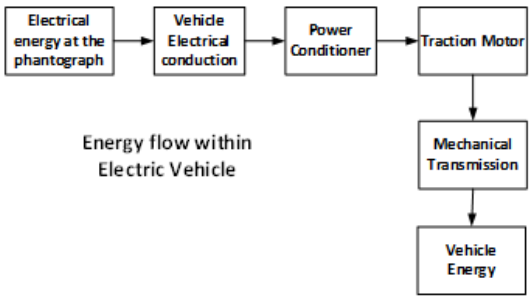

Figure 3 Electric train Energy flow block

Train electrical conductors

Electric energy is transported by electric conductors from the pantograph to the electronic power converter, which dissipates heat energy. The cable lengths in the train are usually short and the resistance levels are low, which can be considered as insignificant transmission losses inside the vehicle.

Power conditioner

In order to achieve the necessary torque, the supply of electrical power is controlled by means of power electronic converters. Many new train use induction motors powered by inverter. Inverters transform a DC supply to the VVVF (three-phase variable voltage frequency) supply. Modern inverter consists of six switches (IGBTs with anti-parallel diodes) as shown in Fig.4. The switches are working

to provide the appropriate frequency and voltage for a three-phase AC output.

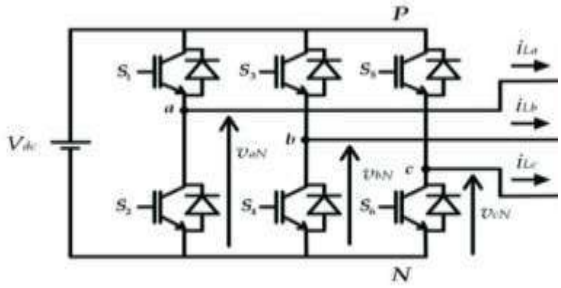

Fig.4 Inverter Circuit Diagram

The loss mechanisms of an inverter can be divided into two categories: conduction and switching [9]. Equation (6) describes the losses in one leg of an inverter P_{ILLs}

$$P_{ILLs} = P_{cD} + P_{cQ} + P_{s,onQ} + P_{s,offQ} \quad (6)$$

where P_{cD} =conduction losses in the diodes

P_{cQ} = conduction losses in the IGBTs

$P_{s,onQ}$ = switch-on losses in the IGBTs

$P_{s,offQ}$ = switch-off losses in the IGBTs

The diode conduction, P_{cD} losses can be described as

$$P_{cD} = \frac{1}{T}\int_0^T V_\alpha(t) i_\beta(t) dt \quad (7)$$

where $V_\alpha(t)$ is the diode junction voltage an $i_\beta(t)$ is the diode current, when the diode conducts this equals the line motor current. $V_\alpha(t)$ can be written as a function of the current as shown below,

$$V_\alpha(t) = V_{\alpha o}(t) + i(t) R_\delta \quad (8)$$

The values for $V_{\alpha o}(t)$ and R_δ can be derived [9] from manufacturer's datasheets [10]. For a Siemens BSM75GB120 these values are $V_{\alpha o}(t)$ = 1.25V and R_δ = 7.71$m\Omega$. The IGBT conduction losses can be described as

$$P_{cQ} = \frac{1}{T}\int_0^T V_\psi(t) i_\varsigma(t) dt \quad (9)$$

where, $V_\psi(t)$ is the IGBT junction voltage and $i_\varsigma(t)$ is the IGBT forward current, which equals the motor current, when the IGBT is conducting, $V_\psi(t)$ varies is a function of the current.

$$V_\psi(t) = V_{\psi o}(t) + i_\varsigma(t) R_\psi \quad (10)$$

where $V_{\psi o}$ is 1.83V and R_ψ is 17.33$m\Omega$ [10]. The switching losses, γ_{on} and γ_{off} are a function of the IGBT forward current. Fig.5 shows the switching losses for a Siemens device, BSM75GB120.

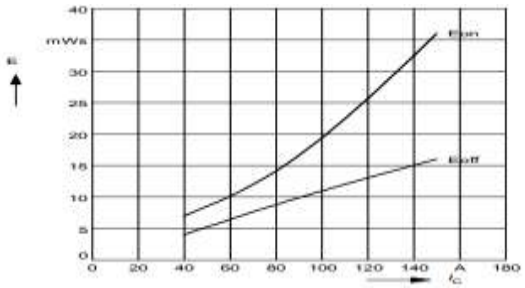

Fig.5 Switching losses against current for aSiemens BSM75GB120 device [10]

The energy loss over one cycle is the sum of the energy losses from each switching operation. The switching losses vary over the sine wave. To simplify the calculation, the RMS current is used to find the switch on and switch off losses from the graph. The switching power (P_s) can be described as.

$$P_s \approx \varepsilon_\phi(\gamma_{on} + \gamma_{off}) \quad (11)$$

The inverter loss energy is dissipated as heat, and therefore there is a cooling requirement. For the purpose of analyzing energy flows, the gate drive control circuit and cooling energy requirements are considered as auxiliary loads.

The induction motor

Induction motor loss mechanisms include ohmic losses, iron losses and frictional and wind age losses [11]. The frictional and wind age losses can be considered as part of the train's frictional loss. When the coefficients of the Davis equation are determined, the motor frictional and wind age losses are included in the tractive resistance analysis. The ohmic losses that occur in the stator and rotor and are dependent on the stator and rotor resistances,

R_ϕ and R_θ and stator and rotor RMS currents, i_ϕ and i_θ.

$$P_\Omega = i_\phi^{\,2} R_\phi + i_\theta^{\,2} R_\theta \quad (12)$$

There are three iron losses, P_{iron}, mechanisms, Hysteresis loss P_{hyst}^{D}, eddy current loss, P_{eddy}^{D} and anomalous loss, P_{anom}^{D}. Iron losses can be simplified and related to the magnetization current.

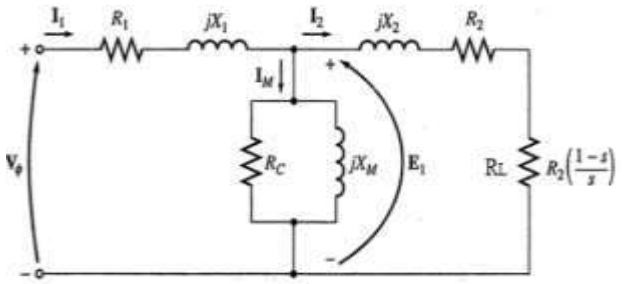

Fig.6 Induction Motor Equivalent Circuit [12]

An induction motor can be represented as a quasi-steady state equivalent circuit, Fig.6, using resistances to represent the three loss mechanisms, R_s, R_r and R_c, representing the stator copper loss, the rotor copper loss and the iron loss respectively. The equivalent circuit can be evaluated to determine the motor losses.

Mechanical transmission

The final stage of the drive is the mechanical transmission. The transmission consists of a gear box, usually made of up a driver gear on the motor shaft and a gear on the axle. Losses occur when one gear drives another [13]. The losses can be related to the coefficient of friction, υ.

$$P_\sigma = P_\tau \left[\frac{\upsilon'}{2} (\lambda_\alpha^{\,2} + \lambda_\beta^{\,2}) \right] \quad (13)$$

where P_τ is the mechanical power transmitted, λ_α is the angle of approach for the driver gear and λ_β is the angle of recess for the driver gear. Frictional losses of the mechanical transmission, including bearing losses are considered as part of the frictional losses of the train. If frictional coefficients are determined using rundown tests, the effects of friction within the drive line are considered.

Auxiliary loads

In general, this includes the auxiliary energy needed for the ventilation of traction motors and the traction converter cooling, but also includes the operation of the brake system for the vehicle (e.g., compressed air). As far as passenger vehicles are concerned, there is an additional energy demand to ensure passenger comfort, such as heating, lighting, and coach ventilation. This energy, which typically accounts for about 20% of the total energy consumption of a train, is supplied by the primary energy source used for traction (catenary or diesel) and delivered along the train by the auxiliary bus supply distribution [14-15].

Traction power supply system and losses

In electrified traction systems, vehicles are powered by electricity which is supplied from a local distribution network through a traction supply system. For the purpose of analyzing the energy flows of an electrified transit system, energy flows in the electricity supply system are considered from the point of connection to the local distribution system. The traction electrical supply system includes the traction substations, the conductor system and a contact system. For DC systems, substations are located every few kilometers along the system (depending on the systems utilization and the voltage level). Substations consist of a transformer and a rectifier. Typically, 12-pulse rectifiers are used to reduce harmonic distortion on the local distribution network. Fig.7 shows a traction substation layout [16]. Transformer losses are divided into two categories, copper losses in the windings and core losses (P_c) due to hysteresis and eddy currents losses [17]. These loss mechanisms are similar to those described for induction motors.

$$P_\chi = 3(i_1^{\,2} R_1 + i_{2\alpha}^{\,2} R_{2\alpha} + i_{2\beta}^{\,2} R_{2\beta}) + P_c \quad (14)$$

where $R_1, R_{2\alpha}$ and $R_{2\beta}$ represent the resistance of the primary winding, and wye and delta windings of the secondary respectively. $i_1, i_{2\alpha}$ and $i_{2\beta}$ represent the primary and two secondary currents respectively. To simplify the equation an equivalent resistance can be used to relate the copper losses (P_χ) to the output current of the substation, i_κ

$$P_\chi = i_\kappa{}^2 R_{e\kappa} + P_c \quad (15)$$

A 12-pulse rectifier consists of two full bridge rectifiers; each bridge contains of six diodes. At any instant four diodes are conducting, hence the losses of the rectifier can be determined by considering the losses in four diodes. Diode power losses occur due to the forward bias voltage (V_ξ). The forward bias voltage varies with current, and can be described as

$$V_\xi = V_{\xi o}(t) + iR_\xi \quad (16)$$

These values can be derived from manufacturers data sheets, for a diode rectifier $V_{\xi o} = 0.81$ V and $R_\xi = 4.8$ m Ω, [10]

$$P_\xi(t) = V_{\xi o} i_\xi + i_\xi{}^2 R_\xi \quad (17)$$

The four diodes that are conducting each conduct the rated current. The power loss in the rectifier (P_ω) can be described as,

$$P_\omega = 4V_\xi i_\kappa + 4R_\phi i_\kappa{}^2 \quad (18)$$

where i_κ is the substation output current. The overall loss of the substation is determined by adding the transformer losses to the rectifier losses and can be described as a quadratic function of the substation current.

$$P_\kappa = i_\kappa{}^2 (R_{2e\kappa} + 4R_\phi) + 4V_\xi i_\kappa + P_c \quad (19)$$

The power loss can be related to the substation power, P_κ

$$P_\kappa = i_\kappa{}^2 \left(\frac{R_{2e\kappa} + 4R_\phi}{v^2}\right) + \frac{4V_\xi}{v^2} p_{s\kappa} + P_c \quad (20)$$

This is integrated to calculate the energy dissipated.

$$P_\kappa = \int_{t_o}^{t} \left(i_\kappa{}^2 \left(\frac{R_{2e\kappa} + 4R_\phi}{v^2}\right) + \frac{4V_\xi}{v^2} p_{s\kappa} + P_c\right) dt \quad (21)$$

Power is transmitted from the traction substations to the vehicles through a conductor system, for light rail systems this is usually an overhead line catenary, some metro systems use conductor rails. Energy is dissipated through I^2R losses in the conductors. Fig. 16 shows a double end fed section, with a single vehicle. Current is supplied from both substations through resistances R_{sA} and R_{sB}, and returns through R_{RA} and R_{RB}. The transmission losses in this system can be

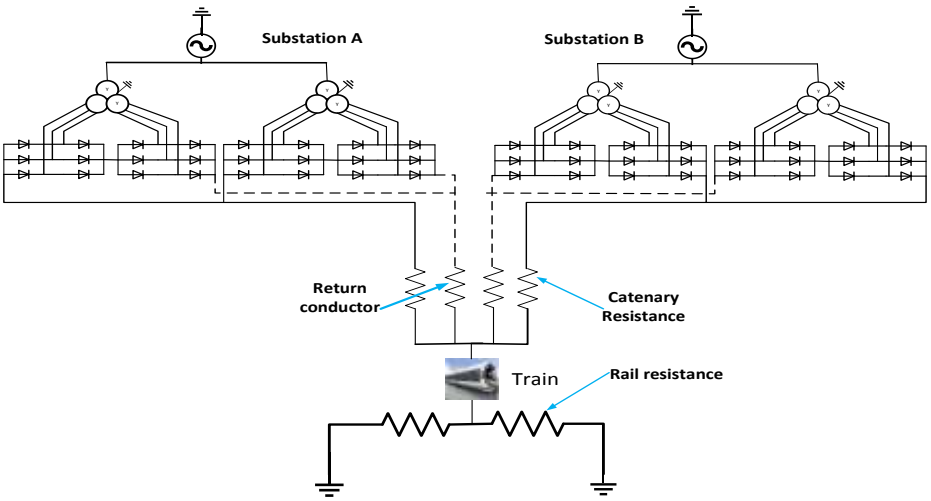

Fig.7 Addis Ababa light rail transit traction power supply network [16]

described by adding the losses in each length of conductor.

$$P_{sL} = i_{sA}{}^2 R_{sA} + i_{sB}{}^2 R_{sB} + i_{RA}{}^2 R_{RA} + i_{RB}{}^2 R_{RB} \quad (22)$$

This can be generalized for any system and described as the sum of copper losses:

$$P_{sL} = \sum i_n{}^2 R_n \quad (23)$$

where i_n is the current and R_n is the resistances of sections of the supply system. To consider the energy loss, the power loss is integrated over time. The currents and resistances of each section can be described as functions of time, $I(t)$ and R_n(t) respectively.

$$E_{sL} = \int_0^t (\sum i_n{}^2(t) R_n(t)) dt \quad (24)$$

Case study: Addis Ababa light rail transit system

The analysis described in this research paper is applied to the city of Addis Ababa light rail system to determine the distribution of energy dissipation over the drive cycle shown in Fig.8 below.

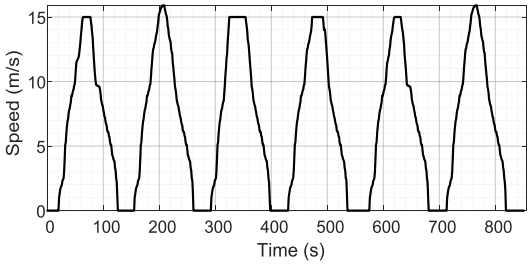

Fig.8 Speed profile of light rail transit system

frictional forces is calculated using equation (25). The case study is based on Addis Ababa light rail transit and therefore the frictional parameters of the light rail can be approximated to those of electric motor train of Addis Ababa. Davis relates the frictional forces for an electric motor train resistance, F_R to the train mass, m (kg), number of axles,n, frontal area A (m^2) and the speed v (m/s).

$$F_R = 0.933\sqrt{mn} + 12700\frac{n}{m} + 8.81.10^{-4} mv + 0.575Av^2 \quad (25)$$

Taking parameters of the Addis Ababa light rail transit (Table 1), the coefficients of the Davis equation can be determined; $a = 481.11$, $b = 38.76$ $c = 5.75$.

Table1. Addis Ababa light rail transit specification [18]

Mass, m	44,000 Kg
Axle, n	6
Frontal area, A	10 m^2
Average speed	15 m/s^2

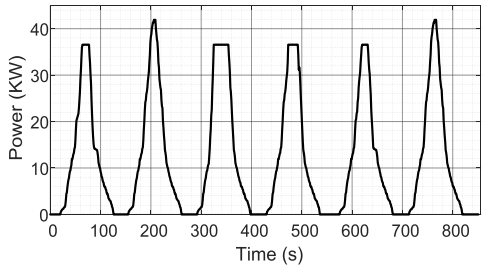

Fig.9 Frictional loss over a simple cycle

Fig.9 shows the friction power profile over drive cycle and found out that 0.551kWh/km energy is dissipated through frictional forces.

Mechanical transmission losses

Gear box losses can be determined by using equation (13), to determine this, the mechanical power, P_τ is required. The mechanical power is the power required to overcome friction and accelerate the vehicle, it is assumed that the vehicle travels on a level track, and hence no energy is required to climb a gradient.

$$P_\tau = P_R + P_\alpha \quad (26)$$

Friction is calculated in the previous section. The power to accelerate the train can be calculated from equations of motion (27).

$$P_\alpha = m.v.\alpha \quad (27)$$

where m is the equivalent mass, which is the sum of the vehicle mass and the equivalent mass of the vehicle rotational parts. The mechanical power for the complete drive cycle is shown in Fig.10.

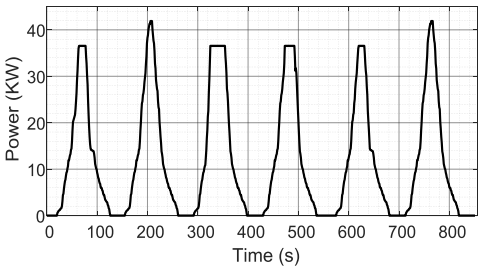

Fig.10 Mechanical power of a single train

The coefficients can be taken from [13] as $\upsilon^{'}$ = 0.0272, λ_{α} =0.3691 rads and λ_{β} = 0.3045 rads. The total energy dissipated through the gears is 0.01kWh/ km. The energy loss profile is shown in Fig.11.

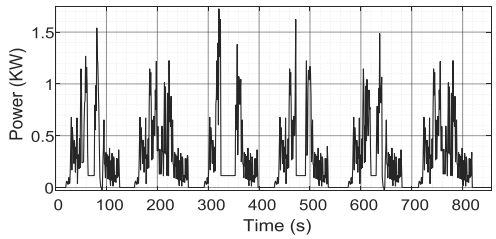

Fig.11 Power dissipated in the gears

The energy dissipated through the gears is small, and so for the purpose of analysis it is added to the frictional losses.

Induction motor losses

The induction motor losses can be divided into three categories; ohmic losses, iron losses, frictional and wind age losses. Frictional and wind age losses are considered as frictional losses of the vehicle. An induction motor can be described as an equivalent circuit as shown in Fig.6. Where $X_r^{'}$ and $R_r^{'}$ are equivalent values. The power dissipated in $R_r^{'}(1-s)/s$ represents the mechanical power generated by the induction motor P_{τ}.

$$P_{\tau} = I_1^{\,2} R_r^{'} \left(\frac{1-s}{s}\right) \tag{28}$$

The mechanical power is equal to the sum of the train mechanical power and the mechanical transmission loss. The power losses in the induction motor can be determined by evaluating the equivalent circuit represented in Fig.6 (for further reference a detail mathematical analysis related to induction motor losses has been performed in [19]).

The power dissipated in the resistances represents the power losses. To determine the power dissipated in the stator and rotor windings, the voltage and frequency of the supply are required. VVVF supply inverters produce a variable voltage variable frequency supply and the voltage is proportional to the frequency.

The equivalent circuit can be solved to determine the losses in each component. The equivalent circuit cannot be solved analytically to determine the required supply voltage and frequency, and therefore the equivalent circuit should be solved numerically, using iterative steps to determine the required voltage and frequency. When the supply voltage and frequency have been determined numerically, the equivalent circuit can be solved to calculate the powers dissipated in each of the equivalent circuit resistors. For a given rotational speed, the motor will have a torque profile depending on the applied frequency and voltage. The torque at a given frequency can be calculated by evaluating the equivalent circuit. The input voltage is proportional to the frequency. The torque can be determined by finding the power dissipated through $R_r^{'}(1-s)/s$ of the equivalent circuit. The rotor circuit can be evaluated by substituting the supply, stator circuit and iron circuit with the venin equivalent supply, Fig.12.

$$v \rightarrow f \tag{29}$$

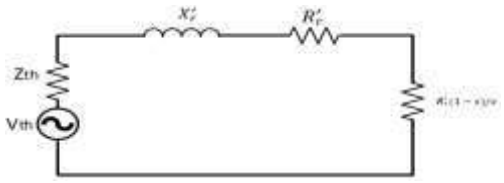

Fig.12 Rotor circuit with a The venin equivalent source

The parameters of the venin equivalent voltage and impedance can be calculated using equations (30) and (31).

$$V_{th} = V_m \frac{\sqrt{x_m^{\,2} + x_c^{\,2}}}{\sqrt{R_m^{\,2} + (x_s + x_m)^2}} \tag{30}$$

$$Z_{th} = R_{th} + jX_{th} = \frac{jx_m(R_s + jx_s)}{R_s + j(x_s + x_m)} \tag{31}$$

The torque T_M produced can be calculated using equation (32)

$$T_M = \frac{3}{\varpi} \frac{V_{th} \frac{R_r}{s}}{(R_{th} + \frac{R_r}{s})^2 + (x_{th} + x_r)^2} \quad (32)$$

Fig.13 shows a motor torque profile at a given rotational speed. The applied motor frequency must lie within the stable region, and hence the minimum and maximum torques should be determined. The minimum and maximum can be determined by sweeping through the frequencies and calculating the torque each time: the point at which torque is at a minimum represents the minimum supply frequency and likewise for the maximum obtainable torque. the solution must lie

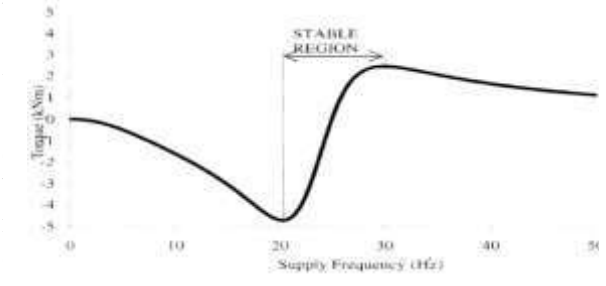

Fig.13 Motor torque profile at 78.5rad/s [20]

calculated torque and the required torque, the error, decreases to an acceptable level. When the supply frequency, and therefore the supply voltage has been determined, the equivalent circuit is solved to find the power dissipated in the stator resistor, rotor resistor and core loss resistor to determine the stator copper loss, the rotor copper loss and the iron core loss respectively.

Table 2. 130 kW motor specifications [21]

Parameters	Values
Stator inductance	0.3121mH
Rotor inductance	0.3121mH
Stator resistance	0.0351Ω
Rotor resistance	0.0211Ω
Magnetizing inductance	1.2mH
Core loss resistance	215Ω

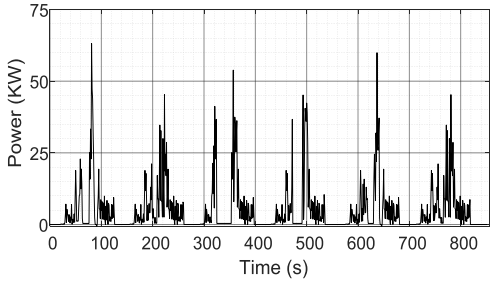

Fig.14 Induction Motor loss for the drive cycle

The total energy dissipated by each induction motor over the drive cycle is 0.083 kWh/km. This gives 0.334 kWh/km for the four induction motors. Fig.14 shows the total motor loss profile for the vehicle.

Power Electronic Converter losses

The induction motor is driven by an inverter. An inverter consists of six IGBTs with anti-parallel diodes. Inverter losses can be divided into two categories, conduction losses (see equations (7-10)) and switching losses (see equation (11)). The conduction loss of an inverter is dependent on the motor current and whether the diode or IGBT is conducting. For the given equations (7) and (9), the values of $V_\alpha(t)$ and $V_\psi(t)$ are, 2.3V and 2.4 V respectively [10]. This means the conduction losses are similar, and so the analysis can be simplified by assuming all the current is conducted by the IGBTs. The conduction loss can be described as a function of the motor current, I_M as shown in equation (34) below,

$$P_{cn} = V_{\psi o} I_m + R_\psi I_m^2 \quad (34)$$

where $V_{\psi o}$ = 1.83 V and R_ψ =I7.73 mΩ. The switching losses depend on the switching frequency, as shown in equation (11). The switching losses both γ_{on} and γ_{off} are functions of current and can be obtained analytically.

They are normally displayed graphically on component datasheets. The relationship can be approximated to a linear relationship as shown in equation (35),

$$P_s \approx \varepsilon_\phi a I_m \quad (35)$$

where a is constant, for Siemens devices this is value is calculated to be 3 x10^{-4} V. The total loss for the inverter can be described as a function of current.

$$P_{ILLs} = V_{\psi o} I_m + R_\psi I_m{}^2 + \varepsilon_\phi a I_m \qquad (36)$$

Taking a switching frequency of 20 kHz and a DC link Voltage of 590 V, the total energy dissipated in each inverter is calculated to be 0.0402 kWh/km. The power electronics driving the motors have a total energy dissipation of 0.16 kWh/Km; Fig.15 shows the power dissipation profile for the power electronics on the vehicle.

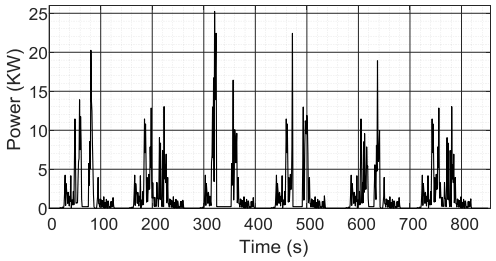

Fig.15 Vehicle Power Electronics Power loss profile

A

The auxiliary load for Addis Ababa light rail transit is assumed constant; measurements have indicated that the average auxiliary load is 15 kW. Over the drive cycle, 0.416 kWh/Km of energy is consumed by the auxiliary loads.

Traction supply system losses

The traction supply system losses can be determined by analyzing the traction supply network. The network impedances are dependent on the position of the vehicle, as the lengths of conductors vary, and hence the parameters of the electrical network vary with time. The losses in the electrical network depend on the total currents, and hence are dependent on all vehicles in the system. Full analysis of system losses should consider all vehicles.

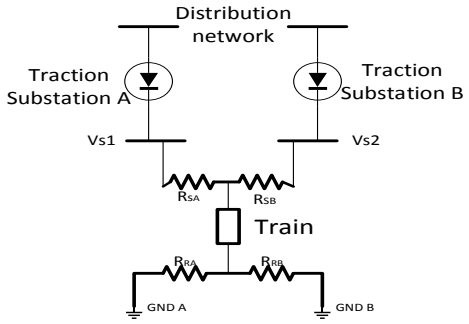

Fig.16 Electrical circuit for a double end fed section of an electrified transit system

To perform the assessment a single train a double end fed section is considered, Fig.16. The section is 1 km long. For the analysis, the train starts in the middle of the section and finishes at the end. The values of the lumped resistances are calculated from the resistance per unit length and the lengths

determined from the position of the vehicle. Values of 0.123 Ω/ km and 0.0924 Ω/km are used for the resistance per unit length of the supply and return conductors respectively [22]. By applying nodal voltage analysis to the system the currents in each section of conductor can be determined. The losses can be determined and summed to find the total transmission loss as shown in equation (23). Fig.17 shows the power loss dissipation profile for the traction supply system and it is found out that 0.034 kWh/km of energy are dissipated in the supply system conductors.

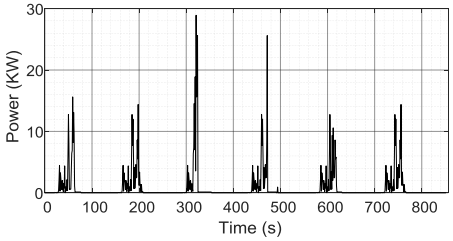

Fig.17 Traction Supply System Losses

The analysis of the traction power supply system network is also used to determine the currents drawn from each substation, which help us to calculate the substation losses. Consequently, equation (19) is used to determine this loss.

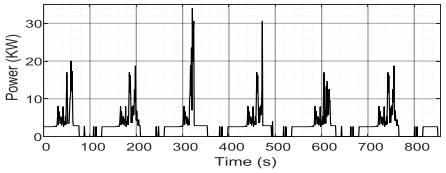

Fig.18 Traction substation losses

Resistance ($R_{2e\kappa}$) (on the DC side), is taken as 0.0233 Ω [19]. R_ϕ is the equivalent resistance of the diodes, V_ξ is the forward bias voltage of the diodes. These values were found to be 0.8 V and 7.7 mΩ respectively [10]. In addition to that the core losses for a 2000 kVA, is 2.6 kW. Finally, the

substation losses are approximated to be 0.236 kWh/Km as shown in Fig.18.

Braking resistor dissipation

During braking, kinetic energy of the vehicle is transferred through the vehicle driveline; the remaining energy is dissipated through braking resistors. The total energy dissipated during the drive cycle is 1.08 kWh/km; Fig.19 shows the braking power profile.

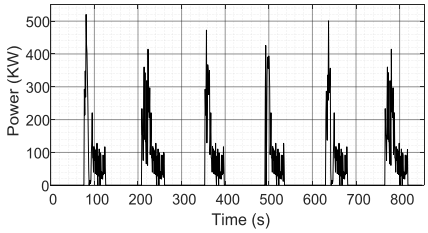

Table 3. Distribution of energy dissipation over the drive cycle.

Components	Energy loss (kWh/Km)	% of total energy loss
Frictional force	0.561	20 %
Induction motor	0.334	11.6 %
Power electronic Devices	0.161	5 %
Auxiliary	0.416	14.5 %
Traction supply losses	0.317	11 %
Braking energy	1.08	37.9 %

Table 3 shows the breakdown of energy loss over a drive cycle. The breakdown only considers the vehicle losses. Based on the analysis it is observed that 37.9 % of total energy dissipates on braking resistor and this tells us that a great deal energy could be saved if energy-storing devices were applied on Addis Ababa light rail system.

CONCLUSIONS

Energy and environmental sustainability are becoming increasingly important as a result of expanding global urbanization. In this sense, compared to other modes of transportation such as road transport, railway plays a major role in lowering energy consumption and CO_2 emissions. Despite its inherent efficiency, the rail industry still consumes a significant amount of energy, making railway energy efficiency a global priority. In this regard, Addis Ababa light rail transit systems also looking for methods to enhance their reliance on sustainable energy. Realizing the above problem, this paper has presented a detailed methodology for analyzing energy flows in a traction system of Addis Ababa light rail transit. The analysis is used to determine the energy dissipated in each component of an electrified transit system. Consequently, the study found out that 37.9% of total energy loss in the traction system is dissipated in braking. This emphasizes the potential of recovering this dissipating energy by using a certain mechanism such as implementing regenerative braking system and energy storage.

REFERENCES

[1]. Rohit Sharma, Peter Newman, Urban Rail and Sustainable Development Key Lessons from Hong Kong, New York, London and India for Emerging Cities, Transportation Research Procedia, Volume 26, 2017,Pages 92-105,

[2]. Sébastien Sauvé, Sophie Bernard, Pamela Sloan, Environmental sciences, sustainable development and circular economy: Alternative concepts for trans-disciplinary research, Environmental Development, Volume 17, 2016,Pages 48-56,

[3]. Jonas Åkerman, Anneli Kamb, Jörgen Larsson, Jonas Nässén, Low-carbon scenarios for long distance travel 2060, Transportation Research Part D: Transport and Environment, Volume 99,2021.

[4]. Katalin Bódis, Ioannis Kougias, Arnulf J ger Waldau, Nigel Taylor, Sándor Szabó, A highr esolution geospatial assessment of the roof topsolar photovoltaic potential in the European Union, Renewable and Sustainable Energy Reviews, Volume 114, 2019.

[5]. EVENT Evaluation of Energy Efficiency Technologies for Rolling Stock and Train Operation of Railways," Institute for Futures Studies and Technology Assessment, Berlin March 2003.

[6]. Williamson, S. Emadi, S. A. and Rajashekara," K. Comprehensive Efficiency Modeling of Electric Traction Motor Drives for Hybrid Electric Vehicle Propulsion Applications," Vehicular Technology, IEEE Transactions on, vol. 56, pp.1561-1572, 2007.

[7]. Zhongbei Tian, Ning Zhao and Stuart Hillmansen "Traction Power Substation Load Analysis with Various Train Operating Styles and Substation Fault Modes" energies, Switzerland, June 2020.

[8]. Kulwora wanichpong, T. Multi-train modeling and simulation integrated with traction power supply solver using simplified Newton–Raphson method. J. Mod. Transport. 23, 241–251 (2015).

[9]. Bai Baodong and Chen Dezhi, "Inverter IGB Tloss analysis and calculation," 2013 IEEE International Conference on Industrial Technology (ICIT), Cape Town, 2013, pp. 563569.

[10]. Siemens Semiconductor Group, "BSM 75 GB120 DN2 Datasheet" [Online]. Available:https://static6.arrow.com/aropdfconversion/26dd3f85945dbe776875a014616b61c5e333cec1/75gb120dn2.accessed February 2020.

[11]. Bulent Sarlioglu, Understanding Electric Motors and Loss Mechanisms, university of Wisconsin Madison, 2016.

[12]. Diaz, A. Saltares, R. C. Rodriguez, R. FNunez, E. I. Ortiz-Rivera and J. Gonzalez Llorente, "Induction motor equivalent circuit for dynamic simulation," 2009 IEEE International Electric Machines and Drives Conference, Miami, FL, 2009, pp. 858-863.

[13]. Buckingham, E. Analytical Mechanics of Gears: Dover Publications, 1988.

[14]. Erik Magni Vinberg, Energy Use in the Operational Cycle of Passenger Rail Vehicles, Master of Science Thesis Stockholm, Sweden2018

[15]. Fisher I. and Bolton G., "Auxiliary power systems for rolling stock," in IEE Eighth Residential Course on Electric Traction Systems, 11-15 Oct. 2004, Manchester, UK,2004.

[16]. Asegid Belay Kebede, Getachew Biru Worku,A research on regenerative braking energy recovery: A case of Addis Ababa light rail transit, transportation, Volume 8, 2021.

[17] Mousavi, S. Shamei M., Siadatan A., Nabizadeh F. and Mirimani, S. H. "Calculation of Power Transformer Losses by Finite Element Method," 2018 IEEE Electrical Power and Energy Conference (EPEC), Toronto, ON, 2018, pp. 1-5,

[18]. China Railway Group (CRECG), Technical Specifications of Vehicles for Addis Ababa light rail transit, internal document, 2011.

[19]. Katsumi Yamazaki, Loss Calculation of Induction Motors Considering Harmonic Electromagnetic Field in Stator and Rotor, Electrical Engineering in Japan, Vol. 147, No.2, 2004.

[20]. Martyn Chymera, the implementation of an energy storage system on-board a light rail traction vehicle, PhD thesis, School of Electrical and Electronic Engineering, john Rylands University, 2019.

[21]. China Railways SS1, Ethiopian light rail transit traction motor detail specification, internal document, 2015.

[22]. Asegid Kebede; Shimelis Atile; Demisu Legese, Harmonic Analysis of Traction Power Supply system: Case Study of Addis Ababa Light Rail Transit, IET Electrical Systems in Transportation, 25 March 2020.